Vol. 620: 119–138, 2019
https://doi.org/10.3354/meps12966

MARINE ECOLOGY PROGRESS SERIES
Mar Ecol Prog Ser

Published June 18

Effects of temperature on the distribution and density of capelin in the Gulf of Alaska

David W. McGowan[1,*], John K. Horne[1], Lauren A. Rogers[2]

[1]School of Aquatic and Fishery Sciences, University of Washington, Seattle, WA 98195, USA
[2]Alaska Fisheries Science Center, National Marine Fisheries Service (NMFS), National Oceanic and Atmospheric Administration (NOAA), Seattle, WA 98115, USA

ABSTRACT: In North Pacific marine ecosystems, Pacific capelin *Mallotus catervarius* are abundant and ecologically important planktivorous fish in pelagic food webs. Environmentally driven changes in their distribution and abundance can affect the availability of capelin to predators, but there is limited information that describes how changes in ocean temperature are related to fluctuations in capelin range and density. A spatiotemporal, generalized linear mixed model was used to quantify the influence of temperature-related covariates on the occurrence and density of age-1+ capelin over the continental shelf in the central and western Gulf of Alaska (GOA) during a period of warm and cold years between 2000 and 2013. Variability in capelin distribution was explained by temperature factors that vary between bathymetric zones. Capelin are predicted to concentrate in moderately stratified waters (i.e. a temperature difference of 3 to 7°C) over shallow banks (<100 m bottom depth) and within deeper troughs (≥100 m). The optimal temperature range for capelin occurrence and catch rates was 8 to 10°C; steep declines occurred in waters warmer than 10.5°C. In contrast to expected northern latitudinal shifts during warm years, capelin shifted northeastward towards the Kodiak Archipelago during the coldest study year, and interannual variation in mean densities was not related to regional mean temperatures. Our findings demonstrate a spatially complex response by capelin to temperature variability over the GOA shelf, and highlight the importance of including potential differences in oceanographic properties among bathymetric zones that may influence distributions of pelagic species.

KEY WORDS: Bathymetry · Diel correction · Forage fish · Habitat · North Pacific · Spatiotemporal · Thermal stratification

1. INTRODUCTION

Climate-related perturbations and long-term warming in the ocean are predicted to affect distributions and abundances of small pelagic fishes (Hollowed et al. 2013a) who modulate the transfer of energy from primary producers to upper trophic species (Pikitch et al. 2012). Capelin *Mallotus* spp. are important small pelagic fishes in boreo-Arctic marine ecosystems, as prey for apex predators and as a commercial species in the Atlantic (Carscadden & Vilhjálmsson 2002). Occurring in all oceans in the Northern Hemisphere at latitudes of ~45 to 80° N (Pahlke 1985, Carscadden et al. 2013a, Logerwell et al. 2015), capelin are distributed from the nearshore to beyond the continental shelf break. Environmentally driven changes in distributions and densities of capelin affect their availability as prey to piscivorous seabirds, marine mammals, and commercially important fish species (Carscadden & Vilhjálmsson 2002, Vilhjálmsson 2002, Ciannelli & Bailey 2005).

Temperature variability and climate-related effects on marine ecosystems have been indirectly and directly associated with fluctuations in distributions and abundances of capelin in the Pacific (Anderson & Piatt 1999, Andrews et al. 2016), Arctic (Carscadden

*Corresponding author: mcgowand@uw.edu

et al. 2013a, Logerwell et al. 2015), and Atlantic (Rose 2005, Carscadden et al. 2013a, Ingvaldsen & Gjøsæter 2013) Oceans. Despite having a wide thermal tolerance (–1.5 to 14°C), small changes in ocean temperatures (~1°C) have been associated with changes in capelin distributions that extend over 100s of km (Rose 2005). Temperature has also been associated with changes in the timing and path of migrations to spawning areas around Iceland (Olafsdottir & Rose 2012, 2013), as well as spawn timing and the selection of spawning habitat in the Northwest Atlantic (Carscadden et al. 1989, Nakashima & Wheeler 2002, Davoren et al. 2012). Distributions and population dynamics of capelin are affected by indirect effects of temperature variability linked to changes in distributions of their predators (Hjermann et al. 2004), and to changes in distributions, abundances, and/or species composition of zooplankton prey (Orlova et al. 2010, Buren et al. 2014).

To maintain thermal habitats, marine fish species are often expected to shift their distributions towards higher latitudes as temperatures increase (Pinsky et al. 2013). Increases in ocean temperature have been associated with a northward shift of capelin around Iceland (Valdimarsson et al. 2012, Carscadden et al. 2013a), similar to observed changes in distributions of demersal fishes in the North Sea (Perry et al. 2005). Likewise, capelin distributions in the Barents and Bering Seas are predicted to shift northward to the Arctic (Huse & Ellingsen 2008, Carscadden et al. 2013a, Hollowed et al. 2013b) in response to projected increases in ocean temperatures and loss of sea ice. In the North Pacific, empirical evidence partially supports predictions of a northward shift corresponding to increases in temperature. The southern range of capelin in the epipelagic zone (<30 m) of the eastern Bering Sea contracted from ~55° N near the Aleutian Islands in cold years to northward of ~60° N (see Fig. 1) in warm years (Andrews et al. 2016). Yet at the same time, recent observations at higher latitudes in the Chukchi and Beaufort seas did not indicate interannual variations in capelin range and relative abundances were influenced by *in situ* ocean temperatures (Logerwell et al. 2015, De Robertis et al. 2017).

Pacific capelin *Mallotus catervarius* (= *M. villosus*, see Mecklenburg et al. 2018), hereafter capelin, are potentially more vulnerable to anomalous warming events (i.e. marine heatwaves) and long-term increases in ocean temperature in the Gulf of Alaska (GOA), where movement north of 60° N is blocked by the Alaska coastline (see Fig. 1). Reduction in capelin abundances in the GOA have corresponded with periods of warm water anomalies in the North Pacific. A regime shift in the late 1970s began a decadal period of warmer ocean temperatures in the GOA (Francis et al. 1998). By the early 1980s, declines in capelin catch rates in shrimp trawl surveys within GOA coastal embayments and reductions of capelin in diets of piscivorous seabirds and marine mammals suggested the GOA population had collapsed (Piatt & Anderson 1996, Anderson & Piatt 1999). The return of relatively cooler temperatures in the northern GOA in the 1990s (Royer & Grosch 2006) coincided with an increase in capelin catch rates in bottom trawl surveys and an expansion of their distribution over the shelf (Mueter & Norcross 2002, Ormseth 2012). More recently, during the 2014 to 2016 North Pacific marine heatwave (Bond et al. 2015, Walsh et al. 2018), multiple surveys observed abrupt declines in capelin densities over the GOA shelf in 2015 and their occurrences in predator diets were also greatly reduced (Zador & Yasumishii 2017, Jones et al. 2017). It is plausible that reductions in suitable thermal habitat may have led to distributional shifts, reduced biomass, and/or collapse of the GOA population. While these observed changes in relative abundance coincided with large-scale (1000s of km) warm water anomalies, the influence of temperature fluctuations on the range and density of capelin at finer scales (10s to 100s of km) remains poorly understood in the GOA.

Temperature is spatially variable over the GOA shelf and not directly related to latitude due to the GOA's complex topography and cyclonic circulation. Numerous fjords and coastal embayments line the GOA's mountainous coastline, while troughs and deep canyons occur on the shelf (Mundy 2005, Zimmermann & Prescott 2015). There are 2 major circulation patterns in the GOA (cf. Fig. 1 in Stabeno et al. 2004): a cyclonic subarctic gyre around the deep basin and the Alaskan Coastal Current (ACC) over the shelf (Ladd et al. 2005, Stabeno et al. 2004, 2016a). The gyre's eastern boundary current advects warm water northward from lower latitudes of the Pacific along the Southeast Alaska coast (Stabeno et al. 2016b). In the northern GOA, the flow turns southwestward where it diverges into the ACC over the shelf and a narrow, high speed western boundary current that runs along the upper slope parallel to the shelf break towards the Aleutian Islands (Stabeno et al. 2004). The ACC is continuous yet highly variable, driven by cyclonic, along-shore winds and freshwater inputs from rivers (Royer 1982, Stabeno et al. 2004, 2016a) that are linked to climate-related atmospheric and oceanographic forcing (Hermann et al.

2016, Stabeno et al. 2016a). The distribution of water masses and spatial patterns of temperature over the GOA shelf are subsequently influenced by fluctuations in the ACC's path and transport. As a result, suitable thermal habitat for capelin over the GOA shelf may not simply contract northward during periods of warm water anomalies; rather, capelin may occupy thermal refuges in deeper water, areas with increased upwelling or vertical mixing, or near tidewater glaciers in coastal embayments (e.g. Arimitsu et al. 2008, 2012).

Capelin are patchily distributed across the GOA shelf but the core of the population is believed to occupy the shelf south and east of the Kodiak Archipelago (see Fig. 1) (Ormseth et al. 2016, Piatt et al. 2018). Compared to other areas of the GOA shelf, waters around Kodiak are highly productive throughout summer (Waite & Mueter 2013, Stabeno et al. 2016a) and this area may function as a summer feeding ground for age-1+ GOA capelin (McGowan et al. 2016). The Kodiak shelf is oceanographically dynamic due to the interaction of the ACC with strong tidal currents and the shelf's complex bathymetry (Stabeno et al. 2016a). While a majority of ACC transport flows to the north of Kodiak down Shelikof Strait and into the western GOA, the remaining transport flows south along the east–southeast side of Kodiak (cf. Fig. 15 in Stabeno et al. 2016a). Therefore, if the availability of suitable thermal habitat over the GOA shelf limits the range and density of capelin, ACC-related variations in the distribution of water masses and temperature are likely to influence variability in capelin distribution and abundance.

We investigated responses of age-1+ capelin to thermal changes in the GOA shelf ecosystem using 7 yr of data collected between 2000 and 2013 in late summer. The objectives of this study were to (1) quantify the influence of temperature on capelin distribution and abundance, (2) quantify interannual shifts in predicted capelin distributions within and between regions of the GOA shelf, and (3) characterize interannual variations in the relative abundance of capelin during warm and cold years.

2. MATERIALS AND METHODS

2.1. Study area and survey design

This study used trawl catch and temperature data from a net-based fisheries oceanographic survey conducted by the Ecosystems and Fisheries-Oceanography Coordinated Investigations (EcoFOCI) program of the National Marine Fisheries Service. The primary objective of the EcoFOCI late-summer, small-mesh trawl survey (hereafter EcoFOCI survey) is to monitor the distribution and abundance of age-0 walleye pollock *Gadus chalcogrammus* (hereafter pollock) prior to the onset of winter. This data has also been used to investigate the influence of oceanographic conditions and zooplankton prey resources on variability in densities of pollock, capelin, and other small pelagic fishes (Wilson et al. 2006, Wilson 2009). Initiated in 2000, the EcoFOCI survey has been conducted biennially during subsequent odd years in late summer (August–September) over the continental shelf in the western GOA (hereafter WGOA) between Shelikof Strait and the Shumagin Islands (Fig. 1). In 2005, a second survey area was added in the central GOA (hereafter CGOA) that sampled the shelf along the southeast side of Kodiak Island. In both regions, the shelf is relatively wide (>200 km) and characterized by complex circulation patterns and bathymetric (e.g. submarine banks, troughs) features (Mordy et al. 2016, Stabeno et al. 2016a). Fixed stations in a grid were occupied to sample fish communities and water properties. Surveys were conducted 24 h d^{-1} by the NOAA Ships 'Miller Freeman' (2000 to 2009) and 'Oscar Dyson' (2013). Of the 8 survey years available from 2000 to 2013, we only analyzed 7. The 2011 survey was excluded from the analysis because it was conducted 1 mo later than the other surveys and only sampled a limited portion of the CGOA region due to logistical constraints.

2.2. Data collection

Trawl and oceanographic samples were collected and processed following Wilson (2009). Briefly, capelin were sampled using a 47 m long Stauffer midwater trawl (cf. Wilson et al. 1996) with a 3 mm codend liner, and fished using 1.5 × 2.1 m steel-V otter doors. Trawls were towed obliquely through the water column at a vessel speed of 1.3 to 1.5 m s^{-1} (2.5 to 3 knots) to a maximum headrope depth of 20 m above the seafloor or 200 m, whichever was shallowest, and retrieved at a rate of 10 m min^{-1}. This sampling depth range covers the vertical distribution of capelin in the GOA (McGowan et al. 2016) Capelin standard length (SL) was measured for up to 100 fish $trawl^{-1}$. Catch per unit effort (CPUE) for capelin biomass density (b, g m^{-2}) for each trawl sample was standardized by:

$$b = W \times \frac{D_{max}}{V} \quad (1)$$

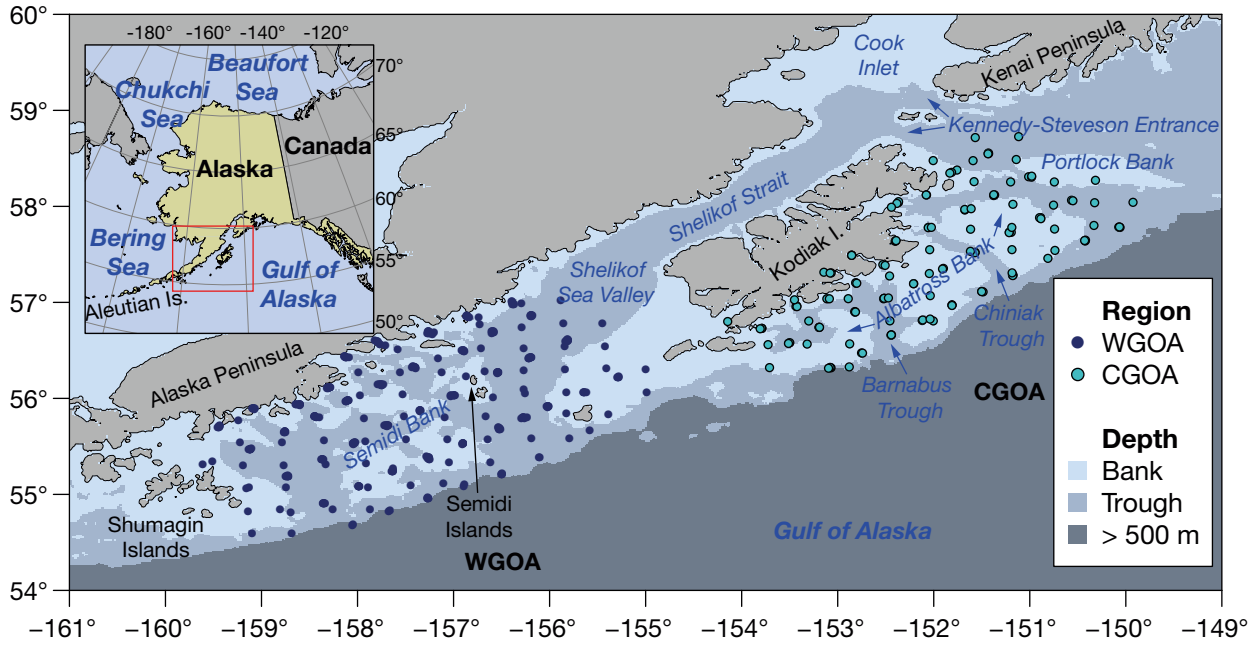

Fig. 1. Capelin survey domain and sample locations by region (WGOA: western Gulf of Alaska; CGOA: central GOA) and bottom depth factor (bank: <100 m; trough: ≥100 m). Red box within inset map: survey domain. Key bathymetric (blue text) and geographic (black text) features mentioned in the text are labeled

where W is the total catch biomass (g), D_{max} is the maximum depth of the trawl (m), and V is the water volume filtered (m^3). V was estimated using mean trawl mouth opening (m^2) and vessel distance (m) traveled between deployment and recovery of trawl doors. Standardization of CPUEs using D_{max} as a multiplier assumes the vessel speed and net retrieval rate remained constant.

Water temperature was measured at each station using a Sea-Bird Electronics (SBE) 19 SeaCat conductivity, temperature, depth (CTD) profiler attached to either a 1 m^2 Tucker trawl (2000 to 2009) or a 60 cm paired bongo net (2013), and deployed within 1 h of the Stauffer trawl. At stations where the SBE 19 SeaCat was not deployed, a temperature profile was sampled using a SBE 39 temperature–pressure recorder attached to the headrope of the Stauffer trawl. Water temperature and pressure (i.e. depth) measurements from the CTD and SBE 39 were used from the up-cast of each tow, and integrated in 1 m depth increments.

2.3. Modeling approach

A geostatistical, delta-generalized linear mixed model (hereafter delta-GLMM) adapted from Thorson et al. (2015b) was used to predict capelin occurrence and positive catch rates (i.e. non-zero densities). A delta (i.e. hurdle) model framework estimates occurrence probabilities separately from estimating catch rates where fish were present (Maunder & Punt 2004):

$$\Pr(B=b)=\begin{cases}1-p & \text{if } B=0\\ p\times Gamma\{b\mid r,\sigma^{-2},r\sigma^{2}\} & \text{if } B>0\end{cases} \quad (2)$$

where the first component of the delta model is a logistic regression that estimates the occurrence probability, p, of non-zero catch rates (i.e. $b > 0$) by fitting a Bernoulli distribution to a binary response B (0, 1) for b. In the second sub-model, positive catch rates, r, are estimated by multiplying p by a probability density function for non-zero catch rates, where σ^{-2} and $r\sigma^2$ are the shape and scale parameters of the gamma distribution, and σ^2 is the catch rate variance.

Following Shelton et al. (2014), the delta-GLMM is a 'semi-parametric' model that includes intercepts for each year, environmental covariates, and random effects for spatial and spatiotemporal covariance (Table 1). Treating spatial and spatiotemporal covariance as random effects enables the use of a stochastic process to represent the cumulative effect of physical and ecological factors on capelin distributions that are not directly measured (Dormann et al. 2007, Thorson et al. 2015c). Both spatial and spatiotemporal covariance are represented by a Gaussian Markov random field (GRF) as:

Table 1. Glossary of indices, covariates, model parameters (fixed and random effects), and estimates used in analysis of capelin density and distribution in the Gulf of Alaska. CPUE: catch per unit effort

Name	Symbol (index)
Indices	
Observation	i
Spatial location (i.e. knot)	s
Year	t
Day–night category (day: >0° solar altitude; night: <−6°)	c
Covariate	k
Covariates	
Observed CPUE (i.e. capelin biomass density, g m^{-2})	$b(i)$
Covariate array	$X(k,s,t)$
Region factor (western and central Gulf of Alaska)	$Reg(s)$
Bottom depth factor (bank: <100 m; trough: ≥100 m)	$fBT(s)$
Standardized mean water temperature (1 to 200 m)	s$Temp(s,t)$
Quadratic term for standardized mean water temperature	s$Temp^2(s,t)$
Water column stratification ($Temp_{1m} - Temp_{btm}$)	s$Strat(s,t)$
Fixed effects (occurrence / positive catch rate)	
Intercept	$\alpha(c,t)/\beta(c,t)$
Covariate effect	$\alpha(k,c)/\beta(k,c)$
Loadings matrix for spatial covariation	$L_\omega^{(p)}(c)/L_\omega^{(r)}(c)$
Loadings matrix for spatiotemporal covariation	$L_\varepsilon^{(p)}(c)/L_\varepsilon^{(r)}(c)$
Decorrelation rate	$\kappa^{(p)}/\kappa^{(r)}$
Positive catch rate variance	$\sigma^2(c)$
Random effects (occurrence / positive catch rate)	
Spatial variation	$\omega^{(p)}(s)/\omega^{(r)}(s)$
Spatiotemporal variation	$\varepsilon^{(p)}(s,t)/\omega^{(r)}(s,t)$
Derived quantities (occurrence / positive catch rate)	
Probability of occurrence	$p(i)$
Positive catch rates	$r(i)$
Spatial covariance matrix	$\Sigma_\omega^{(p)}/\Sigma_\omega^{(r)}$
Spatiotemporal covariance matrix	$\Sigma_{\varepsilon_t}^{(p)}/\Sigma_{\varepsilon_t}^{(r)}$

$$\omega \sim \mathrm{MVN}(0,\Sigma_\omega) \quad (3a)$$

$$\varepsilon_t \sim \mathrm{MVN}(0,\Sigma_{\varepsilon_t}) \quad (3b)$$

where MVN is a multivariate normal distribution centered at 0, Σ_ω is a 2-dimensional spatial covariance matrix of the random field for all spatial locations (i.e. knots, s) following a Matérn distribution with smoothness $v = 1$, and Σ_{ε_t} is the spatiotemporal covariance matrix in year t (Thorson et al. 2015b,c). Covariance between each pair of spatial locations is specified to be stationary and assumed to be isotropic (Thorson et al. 2015c). The stochastic partial differential equation (SPDE) approximation (Lindgren et al. 2011) was used to estimate Σ_ω and Σ_{ε_t}. The 3 components of the precision matrix used in the SPDE approximation (cf. Lindgren et al. 2011) were computed within the R statistical environment (R Core Development Team 2015) using the R package 'INLA' (http://www.r-inla.org; Rue et al. 2009). Values from the random fields for spatial and spatiotemporal covariance were included as random effects in the linear predictors to estimate p and r (described below). The number of spatial locations (n = 190 knots) was determined by the total number of unique grid locations in the survey domain (Fig. 1) that were sampled during at least 2 of the 7 years in the study period. Observations that were not located within 37 km (~20 nautical miles) of another sample from a different year were excluded from the analysis.

Capelin catch rates were examined for potential differences between day and night samples based on prior observations of higher capelin CPUEs at night compared to samples collected during the day in EcoFOCI trawl catches from 2000 to 2003 (Wilson 2009). Sample time of day was categorized into day or night based on solar altitude (Table 1), calculated as a function of location and time using the R package 'oce' version 0.9-21 (https://github.com/dankelley/oce). A solar altitude higher than 0° above the horizon was classified as day, and lower than 6° below horizon (i.e. civil twilight, as defined by the United States Naval Observatory; http://aa.usno.navy.mil/faq/docs/RST_defs.php) was considered night. Similar to Wilson (2009), this preliminary examination of capelin CPUEs showed patterns of higher CPUEs in night samples for all years (for details see Supplement 1; all 4 Supplements are available at www.int-res.com/articles/suppl/m620p119_supp.pdf). CPUEs from limited twilight (0 to −6°) trawl samples (n = 29 out of 552) were highly variable and did not show a clear association with either day or night samples, and were excluded from the analysis.

To account for diel differences in capelin catch rates (see Supplement 1) and to maximize the number of samples included in the analysis, day and night samples were treated as separate categories (hereafter day–night category) within a joint modeling framework (hereafter multi-category, delta-GLMM). Previous studies have adapted the delta-GLMM framework to jointly estimate abundance and range shifts using biomass data for multiple length categories from a single species (Thorson et al. 2017), and multiple species (Thorson et al. 2016). Thorson et al. (2015a) showed that jointly estimating the distributions of multiple rockfish species within a spatial GLMM improved accuracy in predicted

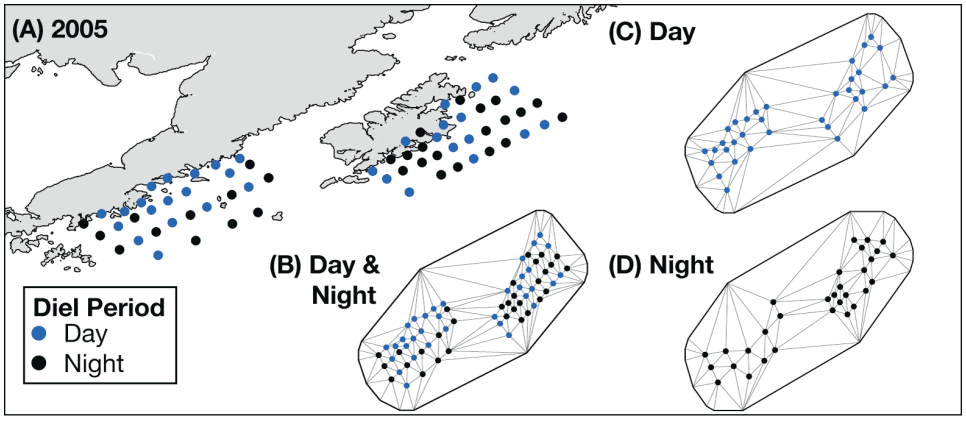

Fig. 2. Example of stations and triangulated meshes used to calculate the precision matrix from which the spatial covariance matrices for Σ_ω and Σ_{ε_t} were derived. Day and night stations from the 2005 survey are used to demonstrate (A) the location of spatial knots within the study area by day–night category and triangulated meshes based on (B) day and night samples, (C) day samples only, and (D) night samples only

catches compared to modeling each species individually. Assuming that the day or night category does not influence spatial correlations related to capelin occurrence and positive catch rates, this study included locations from all day and night samples in the same triangulated mesh (i.e. a triangle vertex located at each spatial knot; Fig. 2) that are generated in the SPDE approximation and used to calculate the precision matrix from which the spatial covariance matrices for Σ_ω and Σ_{ε_t} are derived. Loading matrices were calculated for spatial and spatiotemporal covariation between the day–night categories (Thorson 2019). Parameters for fixed and random effects and derived quantities were estimated separately for each day–night category, sharing only the spatial mesh and decorrelation rate, κ, that is used to calculate the geostatistical range (i.e. the distance at which spatial correlations decline to 10%; Thorson et al. 2015b).

In the delta-GLMM's first sub-model, the p value for sample i was estimated as:

$$p(i) = \text{logit}^{-1}\left(\alpha(c_i,t_i) + \sum_{k=1}^{n_k}\alpha(k,c_i)X_j^{(p)}(k,s_i,t_i) + L_\omega^{(p)}(c_i)\,\omega^{(p)}(s_i) + L_\varepsilon^{(p)}(c_i)\,\varepsilon^{(p)}(s_i,t_i)\right) \quad (4)$$

where $\alpha(c_i,t_i)$ is the intercept for day–night category c in year t for the i^{th} sample, $\alpha(k,c_i)$ is a vector of coefficients estimated as fixed effects of covariates k for day–night category c, $X_j^{(p)}(k,s_i,t_i)$ is a vector of values for covariate combination j (described below) at the spatial location s located nearest to sample i in year t, $L_\omega^{(p)}(c_i)$ and $L_\varepsilon^{(p)}(c_i)$ are fixed effects for the loadings matrix generated for spatial and spatiotemporal covariation for day–night category c, $\omega^{(p)}(s_i)$ and $\varepsilon^{(p)}(s_i,t_i)$ are the values of the random field for spatial and spatiotemporal variation at location s in year t and n_k is the total number of covariates in the model.

In the second sub-model, the r value for sample i was estimated as:

$$r(i) = \exp\left(\beta(c_i,t_i) + \sum_{k=1}^{n_k}\beta(k,c_i)X_j^{(r)}(k,s_i,t_i) + L_\omega^{(r)}(c_i)\,\omega^{(r)}(s_i) + L_\varepsilon^{(r)}(c_i)\,\varepsilon^{(r)}(s_i,t_i)\right) \quad (5)$$

where parameters are defined identically to those used to calculate p in the occurrence sub-model (Eq. 4): β represents coefficients for intercepts and fixed effects of covariates on catch rates in the same way as α, while fixed effects for the loading matrices $L_\omega^{(r)}$ and $L_\varepsilon^{(r)}$, and random effects for spatial $\omega^{(r)}$ and spatiotemporal $\varepsilon^{(r)}$ variation are calculated identically to $L_\omega^{(p)}$ $L_\varepsilon^{(p)}$, $\omega^{(p)}$ and $\varepsilon^{(p)}$ for spatial locations where capelin were present.

The covariate arrays $X_j^{(p)}$ in Eq. (4) and $X_j^{(r)}$ in Eq. (5) include categorical factors and a combination of continuous, temperature-based covariates (Table 1). The categorical factors represented survey region *Reg* with 2 levels (i.e. CGOA or WGOA) and bottom depth *fBT* with 2 levels (i.e. bank or trough, defined in Table 1). Continuous covariates included *in situ* water temperature *Temp* (the mean temperature from the surface to 200 m or 10 m off the bottom, whichever was shallower) and water column stratification *Strat* represented by the difference between water temperature at 1 m and at 200 m or 10 m off the bottom, whichever was shallower. Temperature profiles were averaged for the upper 200 m of the water column to account for uncertainty in capelin vertical distributions during 24 h sampling. Capelin in the CGOA and eastern GOA vary their vertical position relative to bottom depth and occupy a wide range

of depths during daytime (McGowan et al. 2016). The magnitude and direction of capelin diel vertical movements can also vary by year (Mowbray 2002) and age-class (Gjøsæter 1998) in late summer and fall. Therefore, a mean water column temperature was assumed to be a more robust measure of thermal exposure to capelin over a 24 h period compared to measurements from a discrete depth (e.g. surface or bottom temperature). Temperature-based stratification is used as proxy for vertical mixing to identify areas of higher primary productivity (Cheng et al. 2012). To improve model convergence, *Temp* and *Strat* were standardized by subtracting values from their mean and dividing by one standard deviation (indicated by the 's' prefix in the variable name). The effects of s*Temp* and s*Strat* on capelin occurrence and positive catch rates were modeled separately to minimize collinearity between the 2 variables. A quadratic relationship with temperature was modeled by adding an additional s$Temp^2$ term (Bradley & Srivastava 1977).

To account for potential differences in the relative influence of temperature-related covariates on capelin over banks and troughs (McGowan et al. 2018), we included an interaction between the temperature-based covariates with the bottom depth factor *fBT*. Referred to as depth-stratified parameters, coefficients for s*Temp* and s*Strat* were estimated for samples located over banks (<100 m bottom depth), and a separate set of coefficients was estimated for samples in troughs (≥100 m bottom depth). Estimation of depth-stratified parameters accounts for potential differences in oceanographic properties between banks and troughs that influence distributions of capelin. Delta-GLMMs with depth-stratified parameters do not require the same covariate to be estimated for bank and trough samples.

The covariate array X_j for the occurrence and positive catch sub-models was composed of one the following 6 combinations j of covariates k:

$$\begin{aligned}
X_1(k,s,t) &= \{Reg(s), fBT(s), \mathrm{s}Temp(s,t), \mathrm{s}Temp^2(s,t)\}\\
X_2(k,s,t) &= \{Reg(s), fBT(s), \mathrm{s}Strat(s,t)\}\\
X_3(k,s,t) &= \{Reg(s), fBT(s), \mathrm{s}Temp_B(s,t), \mathrm{s}Temp_T(s,t)\}\\
X_4(k,s,t) &= \{Reg(s), fBT(s), \mathrm{s}Temp_B(s,t), \mathrm{s}Strat_T(s,t)\}\\
X_5(k,s,t) &= \{Reg(s), fBT(s), \mathrm{s}Strat_B(s,t), \mathrm{s}Temp_T(s,t)\}\\
X_6(k,s,t) &= \{Reg(s), fBT(s), \mathrm{s}Strat_B(s,t), \mathrm{s}Strat_T(s,t)\}
\end{aligned} \quad (6)$$

where the categorical covariates and *fBT*(s) are indexed at location s, and the standardized continuous covariates s*Temp*, s$Temp^2$, and s*Strat* are indexed at location s in year t. X_{3-6} include depth-stratified terms (i.e. an interaction between s*Temp* or s*Strat* with *fBT*), with the variable subscript indicating whether covariate values are from samples located over banks (e.g. s$Temp_B$) or in troughs (e.g. s$Temp_T$). Due to poor model convergence, depth-stratified parameters were not estimated for the quadratic temperature term (X_{1-2}).

Parameter estimation using maximum marginal likelihood was conducted within the R environment using template model builder (Kristensen et al. 2016) with the R package 'VAST', version 1.1.0 (https://github.com/James-Thorson/VAST; Thorson & Barnett 2017).

2.4. Data analyses

2.4.1. Evaluating single- and multi-category day–night models

Day and night samples were first analyzed separately in single-category, delta-GLMMs with no covariate inputs ($X^{(p)}$ and $X^{(r)}$ set to 0), and then jointly in a multi-category, delta-GLMM to assess differences in model performance. Differences between the single- and multi-category models were assessed by comparison of variance parameters for fixed and random effects (Table 1) and evaluation of model fits by visually inspecting diagnostic plots of both components of the delta model. Model diagnostic plots included comparison of observed to predicted occurrence p, quantile–quantile (Q–Q) plots, and sign deviance residual scatter plots for positive catch rates (Hardin & Hilbe 2007, Zuur et al. 2009). Observed capelin occurrence was converted from binary values of presence/absence ($b > 0 = 1$, otherwise 0) to a proportion by sorting observations of 0 and 1 by their respective p values in increments of 0.05 and calculating the proportion of samples where capelin were observed to be present within each group (e.g. if 50 observations had a p between 0 and 0.05, and capelin were present in 3 of the 50 observations, the observed occurrence proportion equals 0.06).

2.4.2. Effects of temperature on capelin occurrence and catch rate

Objective 1 examined the influence of temperature-related covariates on capelin occurrence and positive catch rates using the multi-category, delta-GLMM. We assessed 36 candidate models, each containing a different set of the unique covariate arrays (Eq. 6) in the occurrence ($X_j^{(p)}$) and positive catch rate ($X_j^{(r)}$) sub-models. Of the 36 candidate models, 16 included

covariate arrays with depth-stratified parameters for continuous covariates in both sub-models ($X_{3-6}^{(p)} \times X_{3-6}^{(r)}$ = 16 candidate models), 16 included depth-stratified parameters in one of the sub-models ($X_{1-2}^{(p)} \times X_{1-2}^{(r)}$ = 8 models, $X_{3-6}^{(p)} \times X_{1-2}^{(r)}$ = 8 models), and 4 models did not include any interactions with *fBT* ($X_{1-2}^{(p)} \times X_{1-2}^{(r)}$ = 4 models). The best combination of temperature-based covariates among the 36 candidate models was determined using Akaike's information criterion values corrected for finite sample size (AIC_c) (Burnham & Anderson 2002). Visual inspection of diagnostic plots for both components of the delta model was conducted to assess model fit. The explained deviance was also calculated following Zuur et al. (2009) as an additional measure of model performance.

2.4.3. Effects of temperature on distributions and density

Objective 2 quantified interannual shifts in capelin distributions within and between the WGOA and CGOA regions using predicted catch rates from the 'best' model identified in the Objective 1 analysis. Day and night catch rates were normalized to a common scale by dividing values by one standard deviation for the sample's respective day–night category. Center of gravity (CG) and inertia, the mean location of the population and the dispersion of the population around its CG (Woillez et al. 2007), were used to characterize interannual differences in distributions within and between regions. Using normalized, predicted catch rates for all samples, CG and inertia were calculated by year within each region and across both regions using R package 'RGeostats' version 11.1.2 (Renard et al. 2017). Objective 3 characterized interannual variations in the relative abundance of capelin based on the mean predicted catch rate from Objective 1's 'best' model. Annual estimates of capelin mean density were calculated from the predicted catch rates by region and day–night category, and were interpreted as separate indices of capelin relative abundance for day and night within each region.

3. RESULTS

3.1. Data summary

The GOA underwent a period of warming from 2001 to 2005 followed by cooler temperatures (Fig. 3). In the WGOA, mean water column temperatures for the upper 200 m averaged 8.6 ± 0.1°C (mean ± SE) across all 7 yr, varying from a low of 7.6 ± 0.2°C in 2013 to a high of 9.5 ± 0.2°C in 2003. Between 2005 and 2013, the average water temperature was similar in both regions (WGOA: 8.3 ± 0.1°C; CGOA: 8.4 ± 0.1°C), with 2013 also being the coolest year (7.9 ± 0.2°C) in the CGOA and 2005 the warmest (9.4 ± 0.2°C). Temperatures were relatively higher over banks compared to troughs, but the overall warming and cooling pattern observed during the 7 data years was apparent in both bottom depth factor levels.

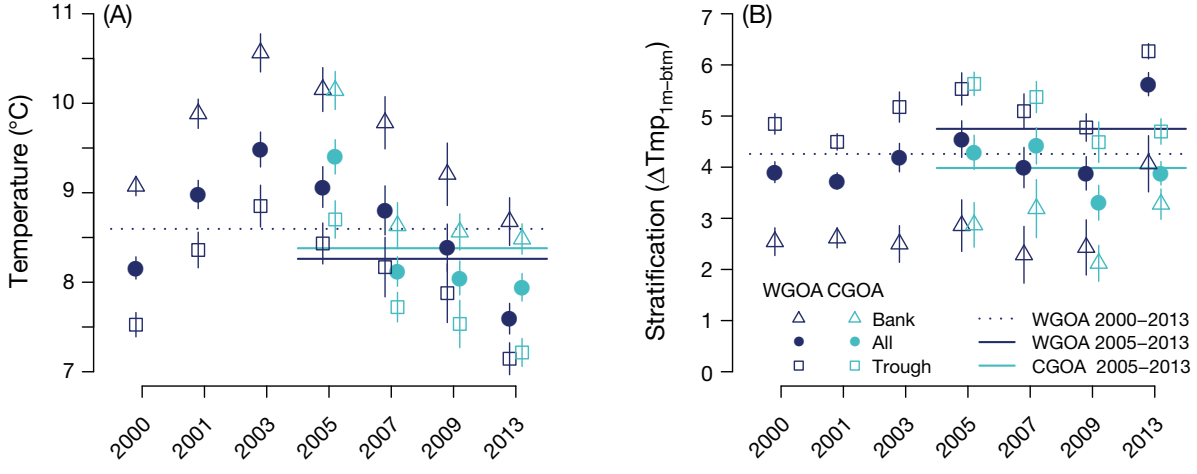

Fig. 3. (A) Observed mean water column temperature and (B) water column stratification by year, region (WGOA: western Gulf of Alaska; CGOA: central GOA), and bottom depth (bank: <100 m; trough: ≥100 m). Values for each year are identified by region and bottom depth factor (all: mean for bank and trough). Horizontal lines: average values for each region for the years shown. Note that mean values were not corrected for potential spatial autocorrelation and standard errors should be interpreted with caution

While temperatures over WGOA banks steadily declined from 2005 to 2013 by 1.5°C, temperatures over CGOA banks dropped by 1.5°C from 2005 to 2007 but then remained within 0.1°C in 2009 and 2013. In contrast, steady declines in temperature occurred in troughs within both regions.

Thermal stratification (i.e. the difference between surface and bottom temperatures) also varied among years (Fig. 3), but was not associated with interannual differences in temperature. In the WGOA, mean stratification values ranged from 3.7 (2001) to 4.5°C (2005) during the first 6 yr that were sampled, but then increased sharply to 5.6°C in 2013. In contrast, mean stratification in the CGOA varied from 3.3°C (2009) to 4.4°C (2007). Waters over banks were relatively less stratified than in troughs by a difference of 1.4 to 2.8°C in annual mean stratification values. Within each bottom depth category, the magnitude of stratification was more than 1°C lower compared to other years in CGOA troughs in 2009 and over CGOA banks in 2009 and 2013, indicating increased mixing of the water column.

A total of 523 trawl samples were analyzed (Table 2). Differences between day–night categories in occurrence (Table 2) and catch rates (Fig. S1.1 in Supplement 1) of capelin occurred between day (n = 289) and night (n = 234) that varied across years, regions, and bottom depth strata. Positive catches were observed more frequently at night (70% of night samples) than during the day (43% of day samples); see Supplement 1 for details.

Capelin lengths ranged from 40 to 142 mm SL (n = 5986), of which 99.5% were longer than 60 mm (Fig. S2.1 in Supplement 2). Based on length–age relationships from Brown (2002), this minimum size indicates that the Stauffer trawl sampled capelin that were 1 yr or older.

3.2. Influence of temperature variability on capelin distributions

The influence of temperature on capelin distributions was quantified using the multi-category, delta-GLMM, which estimates a different set of coefficients for day and night samples. The multi-category model had improved precision and overall model performance compared to the single-category day and night models (details in Supplement 1). Briefly, most spatial variance parameter estimates in the day and night single-category models were higher than the corresponding parameter in the multi-category model or variance was estimated as 0 (indicating the random effects did not contribute to the model) for spatial or spatiotemporal variation (Table S1.1 in Supplement 1). Visual inspection of model diagnostics also showed that the multi-category model had the best fit to both observed occurrence probabilities and positive catch rates (Fig. S1.2). Due to pronounced nonlinear differences in observed CPUEs between day and night samples (Fig. S1.1), predicted catch rates for each day–night category were interpreted as separate indices.

A total of 36 multi-category, delta-GLMMs were analyzed to quantify the influence of temperature variability on capelin occurrence and positive catch rates (Table 3). The candidate model with greatest support based on explained deviance (Model No. 1) included depth-stratified parameters for thermal stratification over banks and temperature in troughs in the occurrence sub-model, and depth-stratified parameters for stratification over banks and in troughs for the positive catch rates sub-model. Model No. 1 explains 54.84% of observed variability in capelin distributions (Table 3). Visual inspection of diagnostic plots shows good fits to both components of the delta-GLMM (Fig. S3.1 in Supplement 3).

Table 2. Number of trawl samples (n) summarized by year for each region (WGOA: western Gulf of Alaska; CGOA: central GOA), bottom depth factor (bank: <100 m; trough: ≥100 m), and day–night category (*D*: day; *N*: night). The proportion of samples with positive catch rates for capelin is indicated within parentheses

Year	WGOA: n = 386 (0.54)				CGOA: n = 137 (0.58)			
	Bank: 145 (0.40)		Trough: 241 (0.63)		Bank: 69 (0.46)		Trough: 68 (0.69)	
	D	*N*	*D*	*N*	*D*	*N*	*D*	*N*
2000	17 (0.47)	17 (0.53)	24 (0.38)	25 (0.76)	–	–	–	–
2001	16 (0.31)	17 (0.41)	26 (0.42)	22 (0.73)	–	–	–	–
2003	13 (0.15)	11 (0.55)	21 (0.71)	20 (0.90)	–	–	–	–
2005	8 (0.25)	3 (1.00)	10 (0.90)	9 (1.00)	9 (0.44)	8 (0.75)	7 (0.57)	11 (0.91)
2007	7 (0.29)	4 (0.75)	8 (0.63)	9 (1.00)	8 (0.25)	6 (0.67)	11 (0.45)	7 (0.43)
2009	10 (0.40)	3 (0.33)	10 (0.70)	11 (0.91)	10 (0.30)	5 (0.60)	7 (0.86)	8 (0.75)
2013	9 (0.11)	10 (0.50)	30 (0.27)	16 (0.38)	18 (0.28)	5 (1.00)	10 (0.80)	7 (0.71)
Total	80 (0.30)	65 (0.52)	129 (0.50)	112 (0.78)	45 (0.31)	24 (0.75)	35 (0.66)	33 (0.73)

Table 3. Model selection results from the multi-category, delta generalized linear mixed model. Candidate models are organized by the inclusion of an interaction between continuous, temperature-based covariates (s*Temp*, s*Strat*) and bottom depth factor (*fBT*; bank: <100 m, trough: ≥100 m) in the capelin occurrence and positive catch rate sub-models. Model numbers indicate their rank relative to corrected Akaike's information criterion (AIC_c) values for all 36 candidate models (see Table S3.1 in Supplement 3). Model structure is indicated by the covariate name listed under each sub-model's bottom depth factor. Sub-models that did not include depth-stratified covariates are centered under both bottom depth factors, and s*Strat* + s$Temp^2$ indicates inclusion of a quadratic term for temperature. The number of parameters are shown for fixed (FE) and random (RE) effects. Model performance is indicated by the explained deviance (Dev)

Model No.	Temperature-based covariates				No. of parameters		Dev (%)
	Occurrence		Positive catch rates		FE	RE	
	Bank	Trough	Bank	Trough			
Both sub-models include depth-stratified parameters							
1	s*Strat*	s*Temp*	s*Strat*	s*Strat*	56	3296	53.83
3	s*Strat*	s*Temp*	s*Strat*	s*Temp*	56	3296	53.40
4	s*Temp*	s*Temp*	s*Strat*	s*Strat*	56	3296	53.35
5	s*Strat*	s*Temp*	s*Temp*	s*Strat*	56	3296	53.32
Only positive catch rates sub-model includes depth-stratified parameters							
2	s*Strat* + s$Temp^2$		s*Strat*	s*Strat*	56	3296	53.66
7	s*Strat* + s$Temp^2$		s*Strat*	s*Temp*	56	3296	53.24
8	s*Strat* + s$Temp^2$		s*Temp*	s*Strat*	56	3296	53.16
16	s*Strat* + s$Temp^2$		s*Temp*	s*Temp*	56	3296	52.50
Only occurrence sub-model includes depth-stratified parameters							
6	s*Strat*	s*Temp*	s*Strat* + s$Temp^2$		56	3296	53.31
12	s*Strat*	s*Temp*	s*Strat* + s$Temp^2$		56	3296	52.84
20	s*Strat*	s*Strat*	s*Strat* + s$Temp^2$		56	3296	52.23
23	s*Strat*	s*Strat*	s*Strat* + s$Temp^2$		54	3296	52.15
Neither sub-model includes depth-stratified parameters							
9	s*Strat* + s$Temp^2$		s*Strat* + s$Temp^2$		56	3296	53.15
26	s*Strat* + s$Temp^2$		s*Strat*		54	3296	51.59
32	s*Strat*		s*Strat* + s$Temp^2$		54	3296	50.76
36	s*Strat*		s*Strat*		54	3296	49.19

Examination of spatial parameter estimates from Model No. 1 indicates that there are important differences between distributions of capelin occurrence and density. Model No. 1 estimated the geostatistical range for capelin occurrence to be approximately 94 km, while distributions of positive catch rates were patchier with a range of 40 km. To assess the stability of capelin spatial patterns, we compared the estimated magnitude of the standard deviations of spatial and spatiotemporal variation within each sub-model (Table 4). In the occurrence sub-model, the standard deviation of spatial variation ($|L_{\omega}^{(p)}{}_{day}|$ = 1.36, $|L_{\omega}^{(p)}{}_{night}|$ = 1.44) was greater than for spatiotemporal variation ($|L_{\varepsilon}^{(p)}{}_{day}|$ = 0.80, $|L_{\varepsilon}^{(p)}{}_{night}|$ = 1.25), indicating that the area occupied by capelin was relatively stable among years. In contrast, spatiotemporal variation ($|L_{\varepsilon}^{(r)}{}_{day}|$ = 1.15, $|L_{\varepsilon}^{(r)}{}_{night}|$ = 1.46) was greater than spatial variation $|L_{\omega}^{(r)}{}_{day}|$ = 0.06, $|L_{\omega}^{(r)}{}_{night}|$ = 0.14) in the positive catch rates sub-model; this shows that there was high interannual variability in distributions of capelin density, which is indicative of a response to changes in environmental conditions (Thorson 2019).

Model No. 1 predicts that occurrence probabilities for capelin increase in waters that are more stratified over banks and relatively warmer in troughs, and that positive catch rates increase in more stratified waters over banks but less stratified waters within troughs (Fig. 4). During both day and night, occurrence probabilities were highest over banks in waters with stratification values that ranged from 2 to 5.5°C, while positive catch rates peaked between 3 and 5.5°C (Fig. 4). In troughs where capelin occupied waters with mean temperatures that ranged from 5.7 to 11.3°C, capelin occurrence probabilities were highest between 7 and 10.5°C, and positive catch rates peaked in waters with stratification values between 3 and 7°C (Fig. 4). Occurrence probabilities are predicted to be higher in troughs compared to over banks during both day (α_{fBT} = 1.32) and night (α_{fBT} = 1.86), while regional differences ($\alpha_{Reg} \leq 0.33$) are relatively less important (Table 4; note the coefficient subscript indicates the covariate name). In contrast, capelin positive catch rates based on day samples are predicted to be higher in the CGOA (β_{Reg} = 1.64), while the regional differ-

Table 4. Parameter estimates (Est) and standard deviations (SD) for the best candidate model (Model No. 1). Subscripts were added to the α_t/α_k and β_t/β_k coefficients to indicate the intercept year/covariate name for each parameter. Parameter estimates are logit transformed in the occurrence sub-model and log transformed in the positive catch rates sub-model. Note the decorrelation rate (κ) is shared by both day–night categories. See Table 1 for parameter definitions; parameters with subscript *B* and *T* indicate a depth-stratified parameter (i.e. an interaction between the covariate with *fBT*, where (*B*) indicates samples from banks (<100 m bottom depth) and (*T*) for samples from troughs (≥100 m)

	Occurrence					Positive catch rates			
Parameter	Day		Night		Parameter	Day		Night	
	Est	SD	Est	SD		Est	SD	Est	SD
α_{2000}	−1.35	0.78	0.49	0.91	β_{2000}	−3.93	0.49	−1.86	0.48
α_{2001}	−1.76	0.79	−0.36	0.92	β_{2001}	−4.22	0.51	−2.56	0.61
α_{2003}	−1.13	0.79	0.51	0.99	β_{2003}	−3.75	0.59	−2.22	0.60
α_{2005}	−0.85	0.80	1.83	1.21	β_{2005}	−2.43	0.57	0.32	0.62
α_{2007}	−1.76	0.85	0.52	1.05	β_{2007}	−1.68	0.64	−0.47	0.63
α_{2009}	−0.79	0.79	1.15	1.08	β_{2009}	−3.32	0.57	−1.19	0.64
α_{2013}	−2.12	0.80	−0.56	0.91	β_{2013}	−4.70	0.62	−1.19	0.62
α_{Reg}	0.31	0.87	0.05	1.07	β_{Reg}	1.64	0.44	−0.07	0.48
α_{fBT}	1.25	0.41	1.37	0.53	β_{fBT}	0.37	0.38	0.30	0.36
α_{sStrat_B}	0.68	0.33	0.96	0.43	β_{sStrat_B}	0.87	0.45	0.71	0.36
α_{sTemp_T}	0.08	0.28	1.18	0.49	β_{sTemp_T}	−0.16	0.20	−0.58	0.21
$L_{\omega}^{(p)}$	−1.36	0.40	−1.44	0.59	$L_{\omega}^{(r)}$	0.06	0.61	−0.14	1.18
$L_{\varepsilon}^{(p)}$	0.80	0.32	1.25	0.59	$L_{\varepsilon}^{(r)}$	1.15	0.27	1.46	0.25
$\kappa^{(p)}$	−3.50	0.34			$\kappa^{(r)}$	−2.64	0.39		
					σ^2	0.09	0.11	0.19	0.09

ence in predicted night catch rates was negligible (β_{Reg} = −0.07; Fig. 4B). Similar to the occurrence sub-model, catch rates are predicted to be higher in troughs during the day (β_{fBT} = 0.37) and at night (β_{fBT} = 0.30). The large standard deviations relative to the β_{fBT} coefficients (Table 4) and lack of apparent differences in predicted catch rates (Fig. 4B) indicate that bottom depth is less important than other covariates when explaining variability in capelin densities. Comparison of day and night parameter estimates supports the assumption that temperature variability similarly influences capelin horizontal distributions during day and night. The sign of coefficients estimated for day and night match for all temperature-based covariates (Table 4).

The influence of stratification on capelin distributions is explained more effectively by estimating a separate linear relationship in banks and troughs (i.e. depth-stratified parameters) compared to models that do not include an interaction with the bottom depth factor (Table S3.1). For example, the explained deviance decreased by 2.08% in Model No. 23 when the effects of stratification on positive catch rates was modeled without the *fBT* interaction. This is not surprising given that Model No. 1 predicted that capelin catch rates increased with stratification over banks but decreased in more stratified waters in troughs (Table 3), with the highest catch rates occurring in waters with stratification values between 3 and 7°C (Fig. 4B).

In contrast to the modeled effects of stratification, the effects of temperature on capelin distributions were better explained by a quadratic relationship compared to a linear relationship for temperature in banks and troughs. For example, comparison of models with the same covariate structure for 1 of the 2 sub-models showed that the explained deviance for Model No. 2 (quadratic temperature in occurrence sub-model) was higher than Model No. 4 by 0.31% (Table 3). Similarly, the deviance was higher by 0.64% for Model No. 6 (quadratic temperature in positive catch rate sub-model) compared to Model No. 15 (Table S3.1). Results for Model Nos. 2 and 6 provide insights into the influence of temperature variability on capelin occurrence and density that cannot be drawn from Model No. 1. Visual inspection of diagnostic plots for Model Nos. 2 and 6 showed each had good fits to both components of the delta-GLMM similar to Model No. 1 (Fig. S3.1). Predicted occurrence probabilities from Model No. 2 (Fig. 5A) and positive catch rates from Model No. 6 (Fig. 5B) show capelin occurrence and catch rates peaked between 8 and 10°C over banks and troughs, but they also show a steep decline in waters warmer than 10.5°C that is not as apparent in Model No. 1 (Fig. 4).

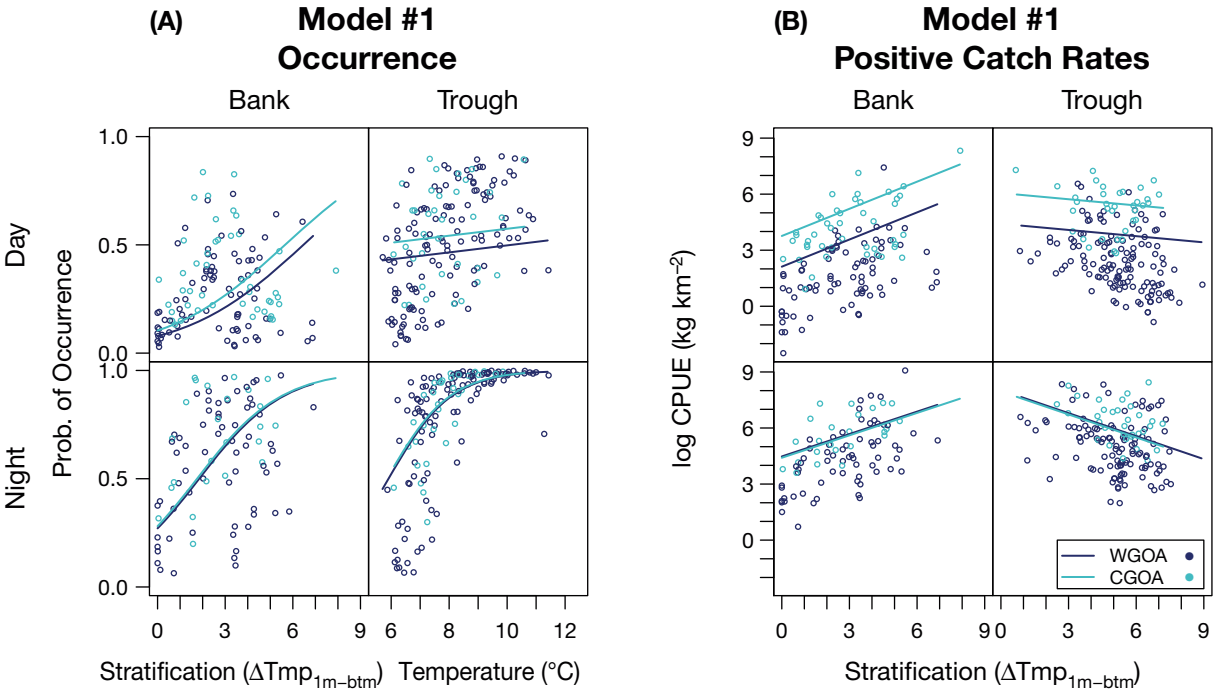

Fig. 4. (A) Predicted capelin occurrence probabilities and (B) positive catch rates (kg km^{-2}) from Model No. 1, the best candidate model, by day–night category, bottom depth factor (bank: <100 m; trough: ≥100 m), and region factor (WGOA: western Gulf of Alaska; CGOA: central GOA). The occurrence model includes depth-stratified covariates for water column stratification over banks and temperature in troughs, and the positive catch rates sub-model includes depth-stratified covariates for stratification over banks and in troughs. Points: predicted values for each sample based on fixed and random effects; lines: predicted values for fixed effects across the range of observed stratification and temperature values based on an average intercept for all years and random effects for spatial and spatiotemporal variation set to 0

3.3. Interannual differences in distributions and density

In all years, distributions of capelin were centered over the inner shelf of both regions (Fig. 6A). High catch rates often occurred near or over edges of banks and were rarely observed over the outer shelf (Fig. S4.1 in Supplement 4). In the WGOA, CGs in all years were located west of the Semidi Islands along the north side of Semidi Bank, with the greatest relative shift occurring to the southeast in 2013. In the CGOA, CGs for all years indicated that capelin were centered over Middle Albatross Bank between Barnabus and Chiniak Troughs. With the exception of 2013 in the WGOA, the long axis of inertia in each year extended parallel to the coastlines of the Alaska Peninsula (WGOA) and southeast side of Kodiak Island (CGOA). In the 4 years that both regions were surveyed, capelin CGs calculated for both regions combined (referred to as GOA) shifted approximately 60 km east and 40 km north in 2013. Contraction of the axes of inertia in 2013 further highlights the low abundance of capelin in the WGOA during that year.

The predicted mean density of capelin in the GOA from Model No. 1 varied between day–night categories, years, and regions (Fig. 7), with a clear increase and decrease in density during the study period. In the WGOA, mean densities were 0.5 to 1.5 orders of magnitude greater at night than during the day. Differences between day and night mean densities were less pronounced in the CGOA, but were at least twice as high at night in 3 of the 4 years. Despite their differences in magnitude, mean densities from day and night in the WGOA were relatively low from 2000 to 2003 and then increased by at least an order of magnitude in 2005. During the day, mean densities in both regions reached a peak in 2007 (mean ± SE: 229.1 ± 97.7 kg km^{-2} in WGOA; 435.2 ± 72.1 kg km^{-2} in CGOA). Daytime mean density declined sharply in the WGOA in 2009 to levels similar to those observed in 2003 and earlier, reaching a minimum of 2.7 ± 0.4 kg km^{-2} in 2013. In the CGOA, relatively high densities persisted through 2009 before similarly declining to a minimum in 2013 of 41.0 ± 8.0 kg km^{-2}. Estimates of mean density for the night index showed a different pattern. In both regions, the night mean density peaked earlier than it did during the day (2005) to

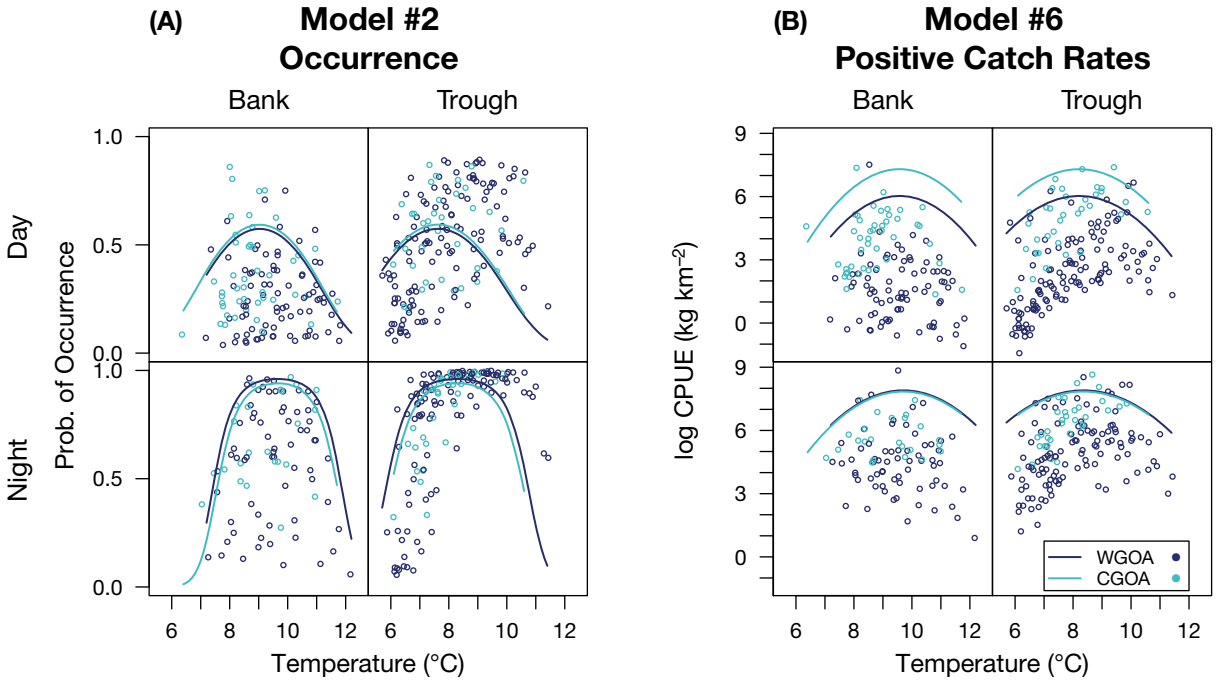

Fig. 5. (A) Predicted capelin occurrence probabilities from Model No. 2 and (B) positive catch rates (kg km^{-2}) from Model No. 6 by day–night category, bottom depth factor (bank: <100 m; trough: ≥100 m), and region factor (WGOA: western Gulf of Alaska; CGOA: central GOA). Both sub-models include effects of a quadratic relationship for temperature on occurrence and positive catch rates. Points: predicted values for each sample based on fixed and random effects; lines: predicted values for fixed effects across the range of observed stratification and temperature values based on an average intercept for all years and random effects for spatial and spatiotemporal variation set to 0

1998.4 ± 626.8 kg km^{-2} in the WGOA and 1240.8 ± 239.9 kg km^{-2} in the CGOA. Mean density in the WGOA remained relatively high in 2007 and then declined in 2009 and 2013. In contrast, mean density in the CGOA dropped to the lowest level in 2007 (434.2 ± 160.5 kg km^{-2}) among the 4 years surveyed, and then increased to 696.9 ± 308.7 kg km^{-2} in 2013.

Some of the variability in this study's mean density estimates may be attributed to the exclusion of 31 twilight samples, including 11 with relatively high catch rates in the WGOA in 2009 and in the CGOA in 2007, 2009, and 2013. For example, the 2007 CGOA mean density estimate may be biased low due to the exclusion of 4 twilight samples located over Albatross Bank whose observed CPUE averaged 540.3 ± 270.1 kg km^{-2}. Nonetheless, we do not believe that inclusion of these samples would significantly alter the observed regional and interannual patterns of relative abundance.

4. DISCUSSION

During warm and cold study years between 2000 and 2013, variability in direct and indirect effects of water temperature influenced the occurrence and catch rates of capelin over the GOA shelf. The response of GOA capelin to temperature variability is complex, as their distributions and densities did not vary as expected for a boreo-Arctic species occupying lower latitudes within its range. Interannual variation in estimates of mean density were not directly related to regional mean temperatures, and distributions shifted northeastward during the coldest study year. Given the wide distribution of capelin across subarctic and Arctic waters, observed movements of GOA capelin are not consistent with *a priori* expectations that this mobile, pelagic species would expand over the GOA shelf during cold years and contract northward in warm years (e.g. Ormseth 2012, Andrews et al. 2016).

4.1. Influence of temperature on capelin distributions

The influence of temperature-based covariates on distributions of capelin was quantified using a multi-category, spatiotemporal delta-GLMM that accounted for differences in capelin CPUEs between day and

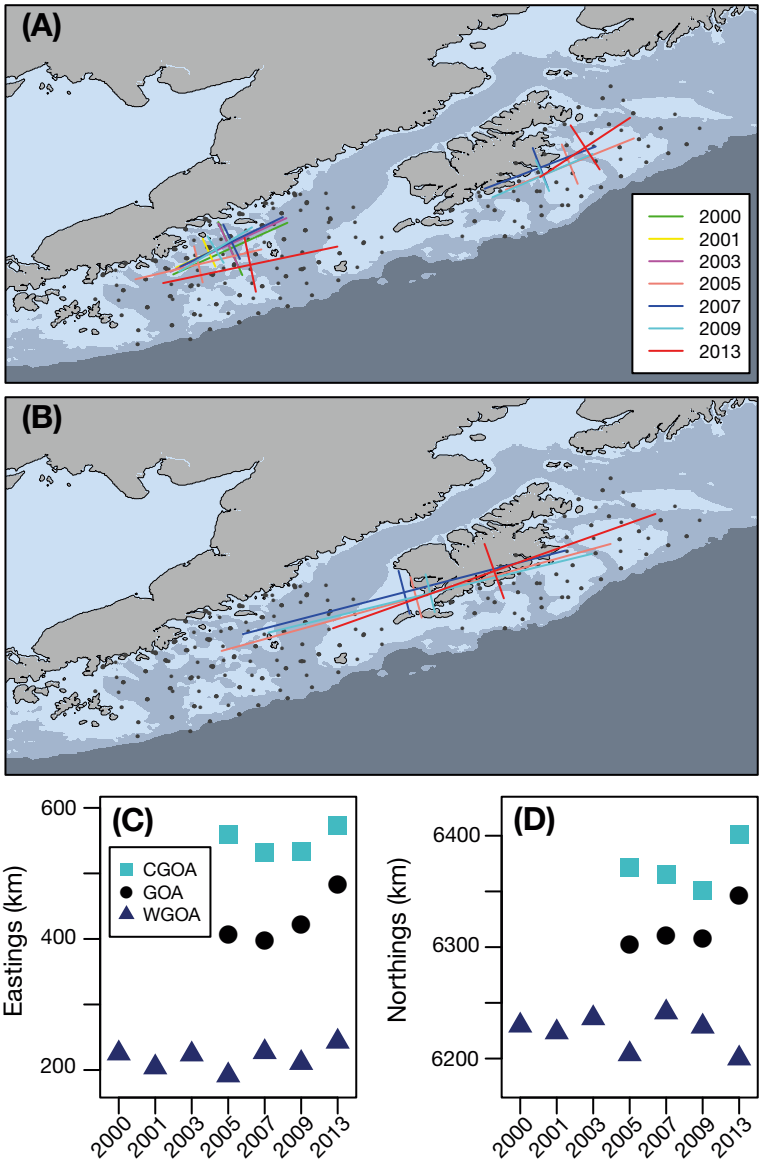

Fig. 6. Center of gravity (line intersection) and inertia (line length) estimates derived from Model No. 1's predicted capelin catch rates by year for (A) samples within each region and (B) samples from both regions combined. Location of center of gravity estimates for each region (WGOA: western Gulf of Alaska; CGOA: central GOA) and both regions combined (GOA) by year along (C) longitudinal ('eastings') and (D) latitudinal ('northings') axes

night. Adapted from Thorson et al.'s (2015a) multi-species model, estimating distributions of capelin simultaneously for day and night categories within a joint modeling framework improved precision of predicted occurrence probabilities and positive catch rates compared to separate models for day and night. This multi-category modeling approach could be adapted for other survey data containing differences in catch rates between day and night samples associated with diel movements and/or species compositions that may mask spatiotemporal changes in distributions.

Model selection results indicated that temperature-related covariates explained variability in capelin distributions over the GOA shelf, but that bio-physical relationships were complex with differences between banks and troughs. Thermal stratification (i.e. the difference between surface and bottom temperatures) best explained capelin occurrence over banks and positive catch rates over banks and in troughs, where the highest densities occur in moderately stratified waters (i.e. a temperature difference of 3 to 7°C). In contrast, the presence of capelin within troughs was best explained by mean water column temperature, with occurrence probabilities peaking between 7 and 10.5°C. Models that estimated the effects of a quadratic relationship for temperature on capelin occurrence and positive catch rates indicated that 8 to 10°C was the optimal temperature range over banks and troughs, and that steep declines in occurrence probabilities and catch rates occurred in waters warmer than 10.5°C.

Thermal stratification can be considered as a measure of vertical mixing (and indirectly, primary production) over the GOA shelf (Stabeno et al. 2016a). Primary production is enhanced at the head of troughs over the GOA shelf due to increased vertical mixing that results from the interaction of tidal currents and the ACC with steep walls along troughs (Mordy et al. 2016, Stabeno et al. 2016a). Predicted increases in capelin catch rates in troughs were associated with reduced thermal stratification, suggesting that capelin concentrate in areas of higher production that results from increased vertical mixing. Over banks, capelin occurrence and positive catch rates were associated with increased thermal stratification. Although this observation is opposite to the predicted relationship in troughs, the result is not surprising given that the magnitude of stratification over banks was much lower than that in troughs, and that strong vertical mixing can potentially inhibit primary production. Intense vertical mixing increases the supply of nutrients from troughs

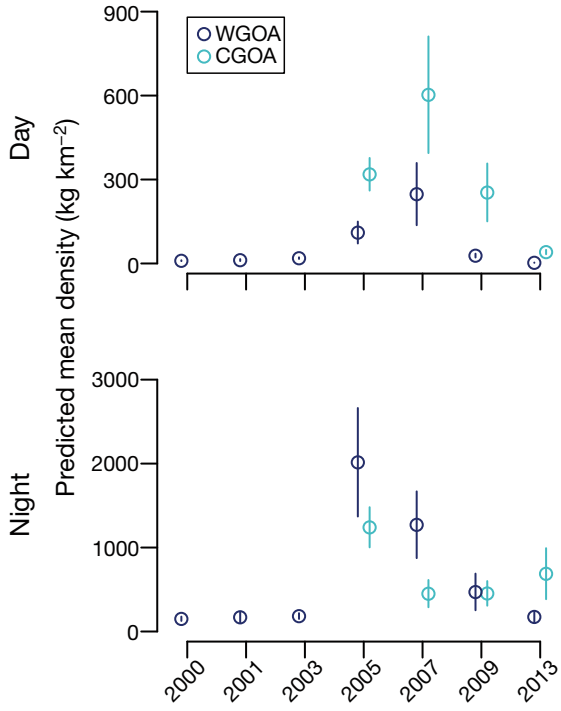

Fig. 7. Annual estimates of predicted mean densities of capelin from Model No. 1 by day–night category and region (WGOA: western Gulf of Alaska; CGOA: central GOA). Vertical lines: estimated SE of the mean. Note that the range of densities is more than 3 times greater at night

to the euphotic zone over banks (Cheng et al. 2012, Mordy et al. 2016), deepens the pycnocline, and reduces phytoplankton densities in the euphotic zone, resulting in lower overall production (Cheng et al. 2012). Adjacent areas that are more stratified with a shallower pycnocline, such as along the edges of banks, would have relatively higher production. These model results, in conjunction with observed distributions, suggest that capelin concentrate over or near the edges of GOA banks in waters with higher localized production. Our findings also highlight the importance of accounting for potential differences in oceanographic properties among bathymetric zones that influence distributions of pelagic species.

The hypothesis that capelin concentrate over or near the edges of GOA banks is consistent with results from McGowan et al. (2018), who showed parallel results using an independent data set. Similar to this study's trough-based observations, McGowan et al. (2018) showed that capelin occupied waters in the CGOA that were associated with warmer bottom temperatures and concentrated in close proximity to the edge of banks (i.e. the 100 m isobath) and in areas with reduced stratification. This study's use of a depth-stratified model was able to differentiate how temperature-based covariates explain variability in capelin distributions in bank and trough habitats that have different oceanographic properties. The expanded domain and duration of this study also demonstrates that the influence of these covariates on capelin distributions is robust across the GOA.

While this study found an influence of temperature on distributions of capelin, additional factors (e.g. physiological condition, prey availability, and predation risk) may also play a significant role. Growth, condition, foraging, distribution, and population abundance of Atlantic capelin have all been shown to vary directly or indirectly with climate-related changes in ocean temperature (e.g. Mowbray 2002, Orlova et al. 2010, Buren et al. 2014). Given a reduction in suitable habitat (Andrews et al. 2016), prey supply (Obradovich et al. 2014), or influx of predators (Hjermann et al. 2004), it is reasonable to assume that capelin will be more likely to occupy waters outside their preferred thermal range if it would increase their net energy intake to optimize growth (MacArthur & Pianka 1966) and/or minimize exposure to predators (Gilliam & Fraser 1987). Further examination of the combined effects of temperature with other factors on distributions and abundances of capelin is needed to better understand the relative importance of mechanisms that influence how GOA capelin respond to different temperature regimes.

4.2. Interannual variability in distributions and density

Although decreases in capelin abundance have previously coincided with warm periods in the GOA (Anderson et al. 1997) and eastern Bering Sea (Andrews et al. 2016), results from this study found a contrasting and less consistent relationship between mean densities and interannual variations in temperature. Annual estimates of mean densities from night catches in the WGOA were both relatively high (2005, 2007) and low (2001, 2003) in warm years, and were surprisingly low during all cold years. In the CGOA, the highest mean density of capelin also occurred during the region's warmest study year (2005), but in contrast to the WGOA, density was relatively high during the coldest year (2013), as well. Overall, interannual variation in mean density was lower in the CGOA compared to the WGOA. Fluctuations in capelin relative abundance appears to be independent of regional temperature in the CGOA, while high abundance in the WGOA only occurred during some (but not all) warm years.

Observed distributions of capelin in this study and other surveys suggest that the CGOA region may comprise core habitat for GOA capelin. The occurrence and density of capelin appears to be relatively more stable in the CGOA, while the WGOA may experience booms and busts in capelin biomass. Capelin were consistently located over Albatross Bank in the 4 survey years examined in this study, and observations from other surveys support the premise that capelin are consistently distributed over the Kodiak shelf. NOAA's Alaska Fisheries Science Center (AFSC) summer bottom trawl survey has observed concentrations of capelin over CGOA banks since the 1990s (Ormseth et al. 2016). Acoustic measurements from 2 independent surveys, the AFSC Midwater Assessment and Conservation Engineering (MACE) Program's summer GOA pollock acoustic-trawl (AT) survey (Guttormsen & Yasenak 2007, Jones et al. 2014) and the Gulf of Alaska Integrated Ecosystem Research Program's (GOAIERP) offshore upper trophic level survey (McGowan et al. 2016), observed aggregations of capelin over CGOA banks and/or within troughs in all years that they were conducted (MACE pollock AT survey: Jun–Aug 2003, 2005, 2011, 2013; GOAIERP: Aug–Oct 2011, 2013). Additional acoustic-trawl surveys of limited spatial coverage in the CGOA from 2000 to 2005 also reported that capelin were consistently observed in Barnabus and Chiniak Troughs (Hollowed et al. 2007, Logerwell et al. 2007, 2010). The consistent presence of capelin aggregations over the CGOA shelf and occurrence in predator diets suggests that the CGOA is an important foraging area for piscivorous groundfish and seabirds (Piatt et al. 2018).

The contrast in mean densities between regions in 2013 (i.e. low in WGOA, moderate-to-high in CGOA) also resulted in the largest change in distributions of capelin northeastward towards Kodiak during the 4 years that were compared. The lack of survey coverage in the northern GOA precludes determining if the observed changes in CG and inertia of capelin distributions in 2013 indicate if the population was displaced to the northeast or had contracted over the CGOA shelf. However, observed high capelin densities in both regions during the warmest year (2005) and low densities of WGOA capelin in the coldest year (2013) contradicts the expectation that capelin distributions would contract (e.g. Andrews et al. 2016) and their abundances would be lower (e.g. Anderson et al. 1997, Sydeman et al. 2017) during warm years. Mean temperatures in 2013 were relatively warmer in the CGOA than in the WGOA. Temperatures in the CGOA can be higher relative to the WGOA due to the GOA's cyclonic circulation that supplies the northern shelf with heat advected northward from the southeast, and then ACC water cools as it flows southwestward due to coastal inputs of snowmelt and cross-shelf intrusions of cold water from the upper slope (Stabeno et al. 2004, 2016a,b). The availability of warmer waters at higher latitudes during a cold year suggests that the thermal envelope and/or other temperature-related factors (e.g. availability and quality of prey, distribution of predators) over the CGOA shelf may have been more suitable for capelin that year. Differences in regional temperatures were reduced in most warmer years, during which suitable thermal habitat for capelin may have been more equally available in both regions.

Given our limited understanding of the processes that influence the distributions and abundances of capelin in the GOA, we propose 4 alternative explanations for the inconsistent relationship between interannual variations in relative abundance of GOA capelin and *in situ* temperature within and between regions: displacement, expansion/contraction, mortality, or recruitment. Displacement of capelin along the GOA shelf, as indicated by interannual differences in mean density between regions, is consistent with observed spatial dynamics for other capelin populations where distribution shifts do not coincide with pronounced changes in the area occupied by a population. For example, in the Barents Sea, increased flux of warm Atlantic water from the west and higher local temperatures coincide with shifts in distributions of capelin to cooler northern and eastern waters (Carscadden et al. 2013a). Observed low mean capelin densities in the WGOA during cold years coincided with high relative abundances of capelin in the northern GOA based on Middleton Island seabird diets (Hatch 2013, Sydeman et al. 2017, Zador & Yasumishii 2017), while the opposite pattern was observed during most warm years from 2000 to 2013. This suggests that capelin distributions may be displaced along the shelf to the northeast during cold years (e.g. 2013) when water temperatures in the GOA may be warmer at higher latitudes, and back to the southwest in warm years (e.g. 2005). Under this scenario, interannual fluctuations in capelin abundance in the CGOA are expected to be less variable relative to variations in other regions.

In contrast, the idea of expansion and contraction of GOA capelin from the Kodiak Shelf is based on observed decadal variability in distributions of capelin catches from the AFSC summer bottom trawl survey (Mueter & Norcross 2002, Ormseth 2012), which showed increases in capelin CPUEs as

the population expanded from the CGOA region across the GOA shelf following the post-regime shift decline in the 1980s (Anderson et al. 1997). If the population is primarily concentrated over the CGOA shelf, as indicated by other survey (Ormseth et al. 2016) and spatially indexed predator diet data (Piatt et al. 2018), one would expect interannual fluctuations in abundance levels in the CGOA to be less variable relative to the WGOA, as observed in this study. Differentiating between displacement and expansion/contraction of the population requires longer time series from the CGOA region and additional data collection from the northern GOA.

Interannual differences in capelin densities between regions may have resulted from shifts in distributions of capelin predators (e.g. groundfish; Yang et al. 2005), resulting in variable capelin mortality and regional abundances. In the eastern Bering Sea, predation on capelin by Pacific cod *Gadus macrocephalus* increased in years when distributions of cod extended further north over the shelf due to northward contraction of a cold water mass (i.e. the cold pool) that cod did not occupy (Ciannelli & Bailey 2005). If movement of capelin between regions over the GOA shelf is limited, increases in predator abundance within one region may impact local capelin mortality and abundance. Observations in the Barents Sea indicate that high predation has impacted the abundance of Atlantic capelin, where poor recruitment occurred in years when influxes of juvenile Atlantic herring *Clupea harengus* from the North Sea resulted in heavy predation on capelin larvae (Hjermann et al. 2004, Carscadden et al. 2013b).

Finally, it is reasonable to speculate that interannual differences in distributions and relative abundances of GOA capelin reflect cumulative mortality incurred during early life stages. Cohort size in Atlantic capelin *Mallotus villosus* populations off Newfoundland and in the Barents Sea are determined by processes that affect mortality during the first year of life (Carscadden et al. 2013b). The timing of capelin spawning is temperature-dependent (Gjøsæter 1998) and varies along GOA beaches from spring through summer (Pahlke 1985). After hatching, capelin larvae are pelagic and likely transported from inshore waters to the GOA shelf by tidal flushing and wind-driven surface currents (Doyle et al. 2002). Over the shelf, larvae are presumed to be advected to the west-southwest by the ACC, similar to other pelagic larvae (e.g. pollock; Parada et al. 2016). Spatiotemporal fluctuations in ACC transport result from variability in alongshore winds and freshwater inputs from rivers (Stabeno et al. 2016a). Therefore, the transport and retention of larvae within the CGOA and WGOA regions is potentially determined by climate-driven processes that influence the timing of spawning and fluctuations in the direction and magnitude of the ACC. For example, satellite-tracked drifter trajectories show that changes in ACC transport through Kennedy-Stevenson Entrance can determine if capelin larvae are advected through Shelikof Strait into the WGOA or are transported southward along the eastern side of Kodiak where current patterns over CGOA banks are favorable for larval retention (Mordy et al. 2016, Stabeno et al. 2016a). Survival of capelin through their first year is also likely influenced by prey availability associated with spatiotemporal variations in primary (Waite & Mueter 2013) and secondary (Coyle et al. 2013) production. Currently, a comprehensive understanding of how early-life stage processes contribute to the spatiotemporal dynamics of age 1+ capelin in the GOA is lacking, and is needed to predict how availability of capelin to predators varies with dynamic environmental conditions and climate regimes in the GOA ecosystem.

Although this study did not detect a clear reduction in suitable habitat for capelin associated with increases in temperature, there are indications that anomalous warm water events or long-term increases in ocean temperatures will impact GOA capelin. Warm water anomalies associated with strong, positive phases of large-scale climate indices (e.g. El Niño Southern Oscillation, Pacific Decadal Oscillation; Zador & Yasumishii 2017) or the North Pacific marine heatwave from 2014 to 2016 (Bond et al. 2015) did not occur during the analyzed time period. During the recent marine heatwave, preliminary analysis of Eco-FOCI trawl survey data from 2015 showed very low capelin densities in CGOA and WGOA regions (Zador & Yasumishii 2017). In addition, low abundance of capelin and other small pelagic fishes in 2015 is believed to have been one of the primary contributing factors to a mass mortality of a capelin predator, common murres *Uria aalge*, in the GOA during the winter of 2015–2016 (Cavole et al. 2016, Walsh et al. 2018). These recent observations, in conjunction with the historical collapse of capelin following the late-1970s regime shift (Anderson & Piatt 1999), supports the hypothesis that capelin are vulnerable to large-scale warm temperature anomalies in the GOA, and that reductions in their abundance subsequently impact the energy flow to predators.

Acknowledgements. We thank Matt Wilson for his leadership of the Ecosystems and Fisheries-Oceanography Coordinated Investigations late-summer midwater trawl survey.

We thank the officers and crew of the NOAA Ships 'Miller Freeman' and 'Oscar Dyson', and members of the scientific parties on EcoFOCI cruises that tirelessly collected survey data over the years. Many thanks to D. Beauchamp, J. Cao, B. Gardner, K. F. Johnson, O. Ormseth, S. Parker-Stetter, E. Phillips, C. Stawitz, and T. Walsworth for insightful conversations about the analysis design. Special thanks to J. Thorson for assistance with the spatiotemporal GLMM. Funding was provided by the North Pacific Research Board and NOAA Fisheries. The manuscript was greatly improved thanks to comments from F. Mueter, L. Ciannelli, and 2 anonymous reviewers. The findings and conclusions in this paper are those of the authors and do not necessarily represent the views of the National Marine Fisheries Service, NOAA. Reference to trade names does not imply endorsement by the National Marine Fisheries Service, NOAA. This research is contribution EcoFOCI-0908 to NOAA's Ecosystems and Fisheries-Oceanography Coordinated Investigations.

LITERATURE CITED

Anderson PJ, Piatt JF (1999) Community reorganization in the Gulf of Alaska following ocean climate regime shift. Mar Ecol Prog Ser 189:117–123

Anderson PJ, Blackburn JE, Johnson BA (1997) Declines of forage species in the Gulf of Alaska, 1972–1995, as an indicator of regime shift. In: Forage fishes in marine ecosystems. Alaska Sea Grant, University of Alaska Fairbanks, Fairbanks, AK, p 531–543

Andrews AG, Strasburger WW, Farley EV, Murphy JM, Coyle KO (2016) Effects of warm and cold climate conditions on capelin (*Mallotus villosus*) and Pacific herring (*Clupea pallasii*) in the eastern Bering Sea. Deep Sea Res II 134:235–246

Arimitsu ML, Piatt JF, Litzow MA, Abookire AA, Romano MD, Robards MD (2008) Distribution and spawning dynamics of capelin (*Mallotus villosus*) in Glacier Bay, Alaska: a cold water refugium. Fish Oceanogr 17: 137–146

Arimitsu ML, Piatt JF, Madison EN, Conaway JS, Hillgruber N (2012) Oceanographic gradients and seabird prey community dynamics in glacial fjords. Fish Oceanogr 21: 148–169

Bond NA, Cronin MF, Freeland H, Mantua N (2015) Causes and impacts of the 2014 warm anomaly in the NE Pacific. Geophys Res Lett 42:3414–3420

Bradley RA, Srivastava SS (1977) Correlation in polynomial regression. Florida State University, Tallahassee, FL

Brown ED (2002) Life history, distribution, and size structure of Pacific capelin in Prince William Sound and the northern Gulf of Alaska. ICES J Mar Sci 59:983–996

Buren AD, Koen-Alonso M, Pepin P, Mowbray F and others (2014) Bottom-up regulation of capelin, a keystone forage species. PLOS ONE 9:e87589

Burnham KP, Anderson DR (2002) Model selection and multimodel inference: a practical information-theoretic approach, 2nd edn. Springer, New York, NY

Carscadden JE, Vilhjálmsson H (2002) Capelin—What are they good for? Introduction. ICES J Mar Sci 59:863–869

Carscadden JE, Frank KT, Miller DS (1989) Capelin (*Mallotus villosus*) spawning on the southeast shoal: influence of physical factors past and present. Can J Fish Aquat Sci 46:1743–1754

Carscadden JE, Gjøsæter H, Vilhjálmsson H (2013a) A comparison of recent changes in distribution of capelin (*Mallotus villosus*) in the Barents Sea, around Iceland and in the Northwest Atlantic. Prog Oceanogr 114:64–83

Carscadden JE, Gjøsæter H, Vilhjálmsson H (2013b) Recruitment in the Barents Sea, Icelandic, and eastern Newfoundland/Labrador capelin (*Mallotus villosus*) stocks. Prog Oceanogr 114:84–96

Cavole LM, Demko AM, Diner RE, Giddings A and others (2016) Biological impacts of the 2013–2015 warm-water anomaly in the Northeast Pacific: winners, losers, and the future. Oceanography (Wash DC) 29:273–285

Cheng W, Hermann AJ, Coyle KO, Dobbins EL, Kachel NB, Stabeno PJ (2012) Macro- and micro-nutrient flux to a highly productive submarine bank in the Gulf of Alaska: a model-based analysis of daily and interannual variability. Prog Oceanogr 101:63–77

Ciannelli L, Bailey KM (2005) Landscape dynamics and resulting species interactions: the cod-capelin system in the southeastern Bering Sea. Mar Ecol Prog Ser 291:227–236

Coyle KO, Gibson GA, Hedstrom K, Hermann AJ, Hopcroft RR (2013) Zooplankton biomass, advection and production on the northern Gulf of Alaska shelf from simulations and field observations. J Mar Syst 128:185–207

Davoren GK, Penton P, Burke C, Montevecchi WA (2012) Water temperature and timing of capelin spawning determine seabird diets. ICES J Mar Sci 69:1234–1241

De Robertis A, Taylor K, Wilson CD, Farley EV (2017) Abundance and distribution of Arctic cod (*Boreogadus saida*) and other pelagic fishes over the US continental shelf of the Northern Bering and Chukchi Seas. Deep Sea Res II 135:51–65

Dormann CF, McPherson JM, Araújo MB, Bivand R and others (2007) Methods to account for spatial autocorrelation in the analysis of species distributional data: a review. Ecography 30:609–628

Doyle MJ, Busby MS, Duffy-Anderson JT, Picquelle SJ, Matarese AC (2002) Early life history of capelin (*Mallotus villosus*) in the northwest Gulf of Alaska: a historical perspective based on larval collections, October 1977–March 1979. ICES J Mar Sci 59:997–1005

Francis RC, Hare SR, Hollowed AB, Wooster WS (1998) Effects of interdecadal climate variability on the oceanic ecosystems of the NE Pacific. Fish Oceanogr 7:1–21

Gilliam JF, Fraser DF (1987) Habitat selection under predation hazard: test of a model with foraging minnows. Ecology 68:1856–1862

Gjøsæter H (1998) The population biology and exploitation of capelin (*Mallotus villosus*) in the Barents Sea. Sarsia 83:453–496

Guttormsen MA, Yasenak PT (2007) Results of the 2003 and 2005 echo integration-trawl surveys in the Gulf of Alaska during summer, Cruises MF2003-09 and OD2005-01. AFSC Processed Rep 2007-04. Alaska Fisheries Science Center, NOAA, National Marine Fisheries Service, Seattle, WA

Hardin JW, Hilbe JM (2007) Generalized linear models and extensions, 2nd edn. Stata Press, College Station, TX

Hatch SA (2013) Kittiwake diets and chick production signal a 2008 regime shift in the Northeast Pacific. Mar Ecol Prog Ser 477:271–284

Hermann AJ, Ladd C, Cheng W, Curchitser EN, Hedstrom K (2016) A model-based examination of multivariate physical modes in the Gulf of Alaska. Deep Sea Res II 132: 68–89

Hjermann DØ, Stenseth NC, Ottersen G (2004) Indirect climatic forcing of the Barents Sea capelin: a cohort effect. Mar Ecol Prog Ser 273:229–238

Hollowed AB, Wilson CD, Stabeno PJ, Salo SA (2007) Effect of ocean conditions on the cross-shelf distribution of walleye pollock (*Theragra chalcogramma*) and capelin (*Mallotus villosus*). Fish Oceanogr 16:142–154

Hollowed AB, Barange M, Beamish RJ, Brander K and others (2013a) Projected impacts of climate change on marine fish and fisheries. ICES J Mar Sci 70:1023–1037

Hollowed AB, Planque B, Loeng H (2013b) Potential movement of fish and shellfish stocks from the sub-Arctic to the Arctic Ocean. Fish Oceanogr 22:355–370

Huse G, Ellingsen I (2008) Capelin migrations and climate change–a modelling analysis. Clim Change 87:177–197

Ingvaldsen RB, Gjøsæter H (2013) Responses in spatial distribution of Barents Sea capelin to changes in stock size, ocean temperature and ice cover. Mar Biol Res 9: 867–877

Jones DT, Ressler PH, Stienessen SC, McCarthy AL, Simonsen KA (2014) Results of the acoustic-trawl survey of walleye pollock (*Gadus chalcogrammus*) in the Gulf of Alaska, June-August 2013 (DY2013-07). AFSC Processed Rep 2014-06. Alaska Fisheries Science Center, NOAA, National Marine Fisheries Service, Seattle, WA

Jones DT, Stienessen SC, Lauffenburger N (2017) Results of the acoustic-trawl survey of walleye pollock (*Gadus chalcogrammus*) in the Gulf of Alaska, June-August 2015 (DY2015-06). Alaska Fisheries Science Center, NOAA, National Marine Fisheries Service, Seattle, WA

Kristensen K, Nielsen A, Berg CW, Skaug H, Bell B (2016) TMB: automatic differentiation and Laplace approximation. J Stat Softw 70:1–21

Ladd C, Stabeno P, Cokelet E (2005) A note on cross-shelf exchange in the northern Gulf of Alaska. Deep Sea Res II 52:667–679

Lindgren F, Rue H, Lindström J (2011) An explicit link between Gaussian fields and Gaussian Markov random fields: the stochastic partial differential equation approach. J R Stat Soc Series B Stat Methodol 73:423–498

Logerwell EA, Stabeno PJ, Wilson CD, Hollowed AB (2007) The effect of oceanographic variability and interspecific competition on juvenile pollock (*Theragra chalcogramma*) and capelin (*Mallotus villosus*) distributions on the Gulf of Alaska shelf. Deep Sea Res II 54:2849–2868

Logerwell EA, Duffy-Anderson J, Wilson M, McKelvey D (2010) The influence of pelagic habitat selection and interspecific competition on productivity of juvenile walleye pollock (*Theragra chalcogramma*) and capelin (*Mallotus villosus*) in the Gulf of Alaska. Fish Oceanogr 19: 262–278

Logerwell E, Busby M, Carothers C, Cotton S and others (2015) Fish communities across a spectrum of habitats in the western Beaufort Sea and Chukchi Sea. Prog Oceanogr 136:115–132

MacArthur RH, Pianka ER (1966) On optimal use of a patchy environment. Am Nat 100:603–613

Maunder MN, Punt AE (2004) Standardizing catch and effort data: a review of recent approaches. Fish Res 70: 141–159

McGowan DW, Horne JK, Parker-Stetter SL (2016) Variability in species composition and distribution of forage fish in the Gulf of Alaska. Deep Sea Res II (in press). https://doi.org/10.1016/j.dsr2.2016.11.019

McGowan DW, Horne JK, Thorson JT, Zimmermann M (2018) Influence of environmental factors on capelin distributions in the Gulf of Alaska. Deep Sea Res II (in press). https://doi.org/10.1016/j.dsr2.2017.11.018

Mecklenburg CW, Lynghammar A, Johansen E, Byrkjedal I and others (2018) Marine fishes of the Arctic region, Vol 1. Conservation of Arctic Flora and Fauna, Akureyri

Mordy CW, Stabeno PJ, Kachel NB, Kachel D, Ladd C, Zimmermann M, Doyle MJ (2016) Appendix 1: importance of canyons to the northern Gulf of Alaska ecosystem. In: The role of cross-shelf and along-shelf transports as controlling mechanisms for nutrients, plankton and larval fish in the coastal Gulf of Alaska. NPRB GOA Project G83 and G85 lower trophic level final report. North Pacific Research Board, Anchorage, AK

Mowbray F (2002) Changes in the vertical distribution of capelin (*Mallotus villosus*) off Newfoundland. ICES J Mar Sci 59:942–949

Mueter F, Norcross B (2002) Spatial and temporal patterns in the demersal fish community on the shelf and upper slope regions of the Gulf of Alaska. Fish Bull 100: 559–581

Mundy PR (2005) The Gulf of Alaska: biology and oceanography. University of Alaska Fairbanks, Alaska Sea Grant College Program, Fairbanks, AK

Nakashima BS, Wheeler JP (2002) Capelin (*Mallotus villosus*) spawning behaviour in Newfoundland waters — the interaction between beach and demersal spawning. ICES J Mar Sci 59:909–916

Obradovich SG, Carruthers EH, Rose GA (2014) Bottom-up limits to Newfoundland capelin (*Mallotus villosus*) rebuilding: the euphausiid hypothesis. ICES J Mar Sci 71: 775–783

Olafsdottir AH, Rose GA (2012) Influences of temperature, bathymetry and fronts on spawning migration routes of Icelandic capelin (*Mallotus villosus*). Fish Oceanogr 21: 182–198

Olafsdottir AH, Rose GA (2013) Staged spawning migration in Icelandic capelin (*Mallotus villosus*): effects of temperature, stock size and maturity. Fish Oceanogr 22:446–458

Orlova EL, Rudneva GB, Renaud PE, Eiane K, Savinov V, Yurko AS (2010) Climate impacts on feeding and condition of capelin *Mallotus villosus* in the Barents Sea: evidence and mechanisms from a 30 year data set. Aquat Biol 10:105–118

Ormseth O (2012) Appendix 2. Preliminary assessment of forage species in the Gulf of Alaska. North Pacific Fishery Management Council, Anchorage, AK

Ormseth O, Moss JH, McGowan DW (2016) Appendix. Forage species report for the Gulf of Alaska. North Pacific Fishery Management Council, Anchorage, AK

Pahlke KA (1985) Preliminary studies of capelin (*Mallotus villosus*) in Alaskan waters. Alaska Department of Fish and Game, Juneau, AK

Parada C, Hinckley S, Horne J, Mazur M, Hermann A, Curchister E (2016) Modeling connectivity of walleye pollock in the Gulf of Alaska: Are there any linkages to the Bering Sea and Aleutian Islands? Deep Sea Res II 132:227–239

Perry AL, Low PJ, Ellis JR, Reynolds JD (2005) Climate change and distribution shifts in marine fishes. Science 308:1912–1915

Piatt JF, Anderson PJ (1996) Response of common murres to the *Exxon Valdez* oil spill and long-term changes in the Gulf of Alaska marine ecosystem. Am Fish Soc Symp 18: 720–737

Piatt JF, Arimitsu ML, Sydeman WJ, Thompson SA and others (2018) Biogeography of pelagic food webs in the North Pacific. Fish Oceanogr 27:366–380

Pikitch EK, Boersma PD, Boyd IL, Conover DO and others (2012) Little fish, big impact: managing a crucial link in ocean food webs. Lenfest Ocean Program, Washington, DC

Pinsky ML, Worm B, Fogarty MJ, Sarmiento JL, Levin SA (2013) Marine taxa track local climate velocities. Science 341:1239–1242

R Core Development Team (2015) R: a language and environment for statistical computing. R Foundation for Statistical Computing, Vienna

Renard D, Bez N, Desassis N, Beucher H, Ors F, Freulon X (2017) RGeostats: the geostatistical R package version 11.1.2. http://rgeostats.free.fr

Rose GA (2005) Capelin (*Mallotus villosus*) distribution and climate: a sea 'canary' for marine ecosystem change. ICES J Mar Sci 62:1524–1530

Royer T (1982) Coastal fresh-water discharge in the northeast Pacific. J Geophys Res 87:2017–2021

Royer TC, Grosch CE (2006) Ocean warming and freshening in the northern Gulf of Alaska. Geophys Res Lett 33: L16605

Rue H, Martino S, Chopin N (2009) Approximate Bayesian inference for latent Gaussian models by using integrated nested Laplace approximations. J R Stat Soc Series B Stat Methodol 71:319–392

Shelton AO, Thorson JT, Ward EJ, Feist BE (2014) Spatial semiparametric models improve estimates of species abundance and distribution. Can J Fish Aquat Sci 71: 1655–1666

Stabeno P, Bond N, Hermann A, Kachel N, Mordy C, Overland J (2004) Meteorology and oceanography of the Northern Gulf of Alaska. Cont Shelf Res 24:859–897

Stabeno PJ, Bell S, Cheng W, Danielson S, Kachel NB, Mordy CW (2016a) Long-term observations of Alaska Coastal Current in the northern Gulf of Alaska. Deep Sea Res II 132:24–40

Stabeno PJ, Bond NA, Kachel NB, Ladd C, Mordy CW, Strom SL (2016b) Southeast Alaskan shelf from southern tip of Baranof Island to Kayak Island: currents, mixing and chlorophyll-a. Deep Sea Res II 132:6–23

Sydeman WJ, Piatt JF, Thompson SA, García-Reyes M and others (2017) Puffins reveal contrasting relationships between forage fish and ocean climate in the North Pacific. Fish Oceanogr 26:379–395

Thorson JT (2019) Guidance for decisions using the Vector Autoregressive Spatio-Temporal (VAST) package in stock, ecosystem, habitat and climate assessments. Fish Res 210:143–161

Thorson JT, Barnett LAK (2017) Comparing estimates of abundance trends and distribution shifts using single- and multispecies models of fishes and biogenic habitat. ICES J Mar Sci 74:1311–1321

Thorson JT, Scheuerell MD, Shelton AO, See KE, Skaug HJ, Kristensen K (2015a) Spatial factor analysis: a new tool for estimating joint species distributions and correlations in species range. Methods Ecol Evol 6:627–637

Thorson JT, Shelton AO, Ward EJ, Skaug HJ (2015b) Geostatistical delta-generalized linear mixed models improve precision for estimated abundance indices for West Coast groundfishes. ICES J Mar Sci 72:1297–1310

Thorson JT, Skaug HJ, Kristensen K, Shelton AO, Ward EJ, Harms JH, Benante JA (2015c) The importance of spatial models for estimating the strength of density dependence. Ecology 96:1202–1212

Thorson JT, Ianelli JN, Larsen EA, Ries L, Scheuerell MD, Szuwalski C, Zipkin EF (2016) Joint dynamic species distribution models: a tool for community ordination and spatio-temporal monitoring. Glob Ecol Biogeogr 25: 1144–1158

Thorson JT, Ianelli JN, Kotwicki S (2017) The relative influence of temperature and size-structure on fish distribution shifts: a case-study on walleye pollock in the Bering Sea. Fish Fish 18:1073–1084

Valdimarsson H, Astthorsson OS, Palsson J (2012) Hydrographic variability in Icelandic waters during recent decades and related changes in distribution of some fish species. ICES J Mar Sci 69:816–825

Vilhjálmsson H (2002) Capelin (*Mallotus villosus*) in the Iceland–East Greenland–Jan Mayen ecosystem. ICES J Mar Sci 59:870–883

Waite JN, Mueter FJ (2013) Spatial and temporal variability of chlorophyll-*a* concentrations in the coastal Gulf of Alaska, 1998–2011, using cloud-free reconstructions of SeaWiFS and MODIS-Aqua data. Prog Oceanogr 116: 179–192

Walsh JE, Thoman RL, Bhatt US, Bieniek PA and others (2018) The high latitude marine heat wave of 2016 and its impacts on Alaska. Bull Am Meteorol Soc 99:S39–S43

Wilson MT (2009) Ecology of small neritic fishes in the western Gulf of Alaska. I. Geographic distribution in relation to prey density and the physical environment. Mar Ecol Prog Ser 392:223–237

Wilson MT, Brodeur RD, Hinckley S (1996) Distribution and abundance of age-0 walleye pollock, *Theragra chalcogramma*, in the western Gulf of Alaska during September 1990. NOAA Tech Rep NMFS 126:11–24

Wilson MT, Jump CM, Duffy-Anderson JT (2006) Comparative analysis of the feeding ecology of two pelagic forage fishes: capelin *Mallotus villosus* and walleye pollock *Theragra chalcogramma*. Mar Ecol Prog Ser 317:245–258

Woillez M, Poulard JC, Rivoirard J, Petitgas P, Bez N (2007) Indices for capturing spatial patterns and their evolution in time, with application to European hake (*Merluccius merluccius*) in the Bay of Biscay. ICES J Mar Sci 64: 537–550

Yang MS, Aydin K, Greig A, Lang G, Livingston P (2005) Historical review of capelin (*Mallotus villosus*) consumption in the Gulf of Alaska and Eastern Bering Sea. NOAA Tech Memo NMFS-AFSC-155

Zador S, Yasumishii EC (2017) Ecosystem considerations 2017: status of the Gulf of Alaska marine ecosystem. North Pacific Fishery Management Council, Anchorage, AK

Zimmermann M, Prescott MM (2015) Smooth sheet bathymetry of the central Gulf of Alaska. NOAA Tech Memo NMFS-AFSC-287

Zuur AF, Ieno EN, Walker NJ, Saveliev AA, Smith GD (2009) Mixed effects models and extensions in ecology with R. Springer, New York, NY

Editorial responsibility: Franz Mueter, Juneau, Alaska, USA

Submitted: July 2, 2018; Accepted: April 12, 2019
Proofs received from author(s): June 7, 2019